Isolation, Characterization And Antibacterial Activity Of Bioinspired Silver Nanoparticles From Bacillus Licheniformis

Ms. Jayshri T. Swami[1], Dr. Nagoba Shivappa N[2*]., Dr. Shivakumar S. Ladde[3]

[1]*Research Scholar, Centre for Research in Pharmaceutical Sciences (CRPS), Channabasweshwar Pharmacy College (Degree), Latur – 413512. swamijayashri520@gmail.com, https://orcid.org/0000-0002-1777-5940*
[2]*Professor and Head, Dept. of Pharmaceutics, Channabasweshwar Pharmacy College (Degree), Latur-413512, Dist. Latur. (MS). nagobashivraj@gmail.com, https://orcid.org/0000-0000-0001-7895-3088*
[3]*Dept. of Pharmacy Practice, Channabasweshwar Pharmacy College (Degree), Latur – 413512. shivkumarladde@gmail.com, https://orcid.org/0000-0001-9011-6354*
**Corresponding Author:*
Dr. Nagoba Shivappa N.
Email: nagobashivraj@gmail.com

Keywords:
Bacillus licheniformis, green synthesis, silver nanoparticles, FTIR, TEM, antimicrobial activity, biogenic nanomaterials.

Abstract
The present study describes a green, cost-effective, and eco-friendly approach for the synthesis of silver nanoparticles (AgNPs) using Bacillus licheniformis isolated from rhizospheric soil. Molecular identification of the isolate via 16S rRNA gene sequencing confirmed its identity with 99.8% similarity to Bacillus licheniformis (GenBank Accession No. LC814576). The biosynthesis of AgNPs was evidenced by a rapid color change from pale yellow to dark brown and further confirmed by a strong surface plasmon resonance (SPR) peak observed at approximately 430 nm using UV–Visible spectroscopy. Fourier-transform infrared (FTIR) spectroscopy revealed the presence of functional groups such as hydroxyl, amide, and carboxyl, indicating the involvement of bacterial metabolites in the reduction and stabilization of AgNPs. Transmission electron microscopy (TEM) demonstrated that the synthesized nanoparticles were predominantly spherical, with a uniform size distribution ranging between 20–30 nm. X-ray diffraction (XRD) analysis confirmed their crystalline nature, showing characteristic peaks corresponding to the face-centered cubic (FCC) structure of silver. Differential scanning calorimetry (DSC) exhibited an exothermic peak at ~102.25 °C, supporting the presence of a stable organic capping layer. The biosynthesized AgNPs exhibited potent antimicrobial activity against multidrug-resistant bacterial pathogens including Staphylococcus aureus, Escherichia coli, Klebsiella pneumoniae, and Pseudomonas aeruginosa. These findings highlight the potential of B. licheniformis as a promising biogenic source for sustainable nanoparticle production with applications in antimicrobial therapeutics and environmental biotechnology.

INTRODUCTION

Nanotechnology has unlocked unprecedented opportunities for developing nanostructured materials with exceptional physicochemical properties. Among these materials, silver nanoparticles (AgNPs) have attracted significant interest due to their wide-ranging applications in medicine, catalysis, environmental remediation, and electronics [1,2]. AgNPs are especially valued for their potent antimicrobial, anti-inflammatory, and antifungal properties, which make them promising tools for addressing antibiotic-resistant infections and microbial contamination [3,4].

However, conventional chemical and physical methods for synthesizing AgNPs pose environmental and health hazards, as they often require toxic reagents and high energy inputs [5,6].

There is thus growing interest in green synthesis approaches that use biological systems as sustainable, eco-friendly alternatives [7,8]. Biological synthesis of nanoparticles harnesses the metabolic capabilities of microorganisms, plants, and fungi to reduce metal ions into nanoscale materials, often capping them with natural biomolecules [9,10]. Bacteria grow rapidly, adapt to diverse environments, and produce a variety of enzymes and metabolites, making them attractive candidates for nanoparticle production. In particular, Bacillus licheniformis, a gram-positive bacterium, has been noted for its extracellular enzymes and ability to produce stable nanoparticles with controlled morphology [8,11].

The rhizosphere, the soil region influenced by plant roots, is a hotspot of microbial diversity and a rich source of bacteria capable of producing bioactive compounds and reducing agents [10,12]. Rhizospheric microbes often produce antimicrobial metabolites to compete in soil ecosystems, making them ideal candidates for green nanotechnology applications. Isolating B. licheniformis from rhizosphere soil thus provides a sustainable avenue for biosynthesizing AgNPs.

This study focuses on the green synthesis of AgNPs using Bacillus licheniformis, aiming to address the dual challenges of sustainability and functional nanoparticle development. The synthesized AgNPs were characterized by UV–Vis spectroscopy, X-ray diffraction (XRD), and transmission electron microscopy (TEM) to determine their structural, optical, and morphological properties. We also evaluated the antimicrobial activity of the bioinspired AgNPs against multidrug-resistant pathogens to assess their potential in combating the global antibiotic resistance crisis [13,14]. By integrating microbial biotechnology with nanotechnology, this research highlights a novel eco-friendly approach for producing functional nanomaterials with broad biomedical and environmental applications.

MATERIALS and METHODS

1. **Collection of Soil Samples:** Soil samples were collected from rhizosphere regions of medicinal garden of Channabasweshwar Pharmacy College (Degree), Latur known for rich microbial diversity. Sampling was conducted at depths of 5–15 cm. Approximately 10 g of soil was collected in sterile containers, transported to the laboratory under aseptic conditions, and stored at 4°C until further processing [10,12].
2. **Isolation and Identification of Bacillus licheniformis:**
    - **Serial Dilution and Plating:** One gram of soil was mixed with 10 mL of sterile saline and subjected to serial dilutions (10^{-1} to 10^{-6}). Aliquots (100 µL) from each dilution were spread on nutrient agar plates and incubated at 37°C for 24–48 hours [15]. Distinct colonies were selected and purified through repeated streaking.
    - **Morphological and Biochemical Characterization:** Purified isolates were characterized using Gram staining, catalase, oxidase, and motility tests [16,17].
    - **Molecular Identification:** Genomic DNA from isolates was extracted using the phenol-chloroform method. The 16S rRNA gene was amplified by PCR using universal primers (Forward: 5'-AGAGTTTGATCCTGGCTCAG-3'; Reverse: 5'-GGTTACCTTGTTACGACTT-3') [18]. Amplified products were sequenced, and sequences were analyzed using NCBI BLAST for species identification. The B. licheniformis strain (SBNN1) was confirmed (Table 1 and Figure 01) and submitted to GenBank (Accession No. LC814576).

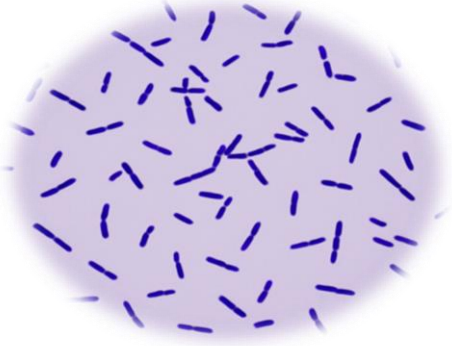

Figure 01: Gram-stained microscopic image of Bacillus licheniformis showing gram-positive, rod-shaped morphology (1000× magnification).

3. **Biosynthesis of Silver Nanoparticles (AgNPs):**
    - **Preparation of Bacterial Supernatant:** B. licheniformis was cultured in Nutient broth at 37°C for 48 hours under shaking (200 rpm). The culture was centrifuged at 10,000 × g for 10 minutes to obtain cell-free supernatant [13].
    - **Synthesis Process:** An aqueous solution of silver nitrate ($AgNO_3$, 1 mM) was mixed with the bacterial supernatant in a 1:1 ratio and incubated in the dark at 37°C for 24–48 hours. AgNP formation was confirmed by a color change from pale yellow to dark brown, indicative of surface plasmon resonance [6,7].
4. **Characterization of Silver Nanoparticles:**
    - **UV–Vis Spectroscopy:** The optical properties of the synthesized AgNPs were analyzed using a UV–Vis spectrophotometer. Absorbance spectra were recorded between 400 and 800 nm to confirm the characteristic surface plasmon resonance (SPR) peak [15].
    - **X-ray Diffraction (XRD):** The crystalline structure of AgNPs was determined using an XRD analyzer with Cu-Kα radiation. Peaks corresponding to the face-centered cubic (FCC) structure of silver were identified [9].
    - **Transmission Electron Microscopy (TEM):** The size and morphology of the AgNPs were analyzed using TEM. Samples were prepared by drop-casting nanoparticle solutions onto carbon-coated copper grids [2].
    - **Fourier-Transform Infrared Spectroscopy (FTIR):** FTIR analysis was performed to identify functional groups involved in nanoparticle formation and capping. Nanoparticle samples were analyzed between 4000–400 cm^{-1} to identify characteristic peaks.

5. Antibacterial Activity Assessment via Agar Well Diffusion Method

The antibacterial activity of synthesized silver nanoparticles (AgNPs) was evaluated using the agar well diffusion technique, as described by Balouiri et al. (19) with slight modifications.

- **Preparation of Mueller–Hinton Agar (MHA) Plates:** Mueller–Hinton agar (MHA) was prepared according to the manufacturer's guidelines. The medium was autoclaved at 121°C for 15 minutes and poured into sterile Petri dishes under aseptic conditions. Plates were allowed to solidify at room temperature and stored at 4°C until use.
- **Preparation of Bacterial Inoculum:** Bacterial strains were subcultured in nutrient broth and incubated at 37°C for 18–24 hours. The bacterial suspension was then adjusted to match the turbidity of a 0.5 McFarland standard, corresponding to approximately 1×10^8 CFU/mL (20).
- **Inoculation of Agar Plates:** Using a sterile cotton swab, the prepared bacterial suspension was uniformly spread over the entire surface of MHA plates to form a confluent lawn.
- **Formation of Wells:** Sterile cork borers (6 mm in diameter) were used to punch wells into the agar at equidistant points. Care was taken to maintain even spacing to prevent overlapping of inhibition zones.
- **Addition of Test and Control Solutions:** Into each well, 50 µL of AgNP solutions at different concentrations (200–500 µg/mL) were pipetted aseptically. A standard antibiotic (e.g., ciprofloxacin) served as the positive control, while sterile distilled water was used as the negative control.
- **Incubation:** All inoculated plates were incubated at 37°C for 24 hours under aerobic conditions.
- **Measurement of Zone of Inhibition (ZOI):** After incubation, the diameter of the clear zones around each well—indicative of bacterial growth inhibition—was measured in millimeters using a digital caliper. All experiments were conducted in triplicate, and the results were reported as mean ± standard deviation.

RESULTS

1. Phylogenetic Identification

The bacterial isolate BL-01 showed 99.8% identity to Bacillus licheniformis based on 16S rRNA gene sequencing (Table 1). A neighbor-joining phylogenetic tree confirmed its close evolutionary relationship (Figure 02 and 03) with other Bacillus licheniformis strains (Accession No. LC814576).

Table 01: BLAST Results for 16S rRNA Gene Sequencing of BL-01

BLAST Hit	Accession No.	Identity (%)	Query Coverage (%)
Bacillus licheniformis	NR_118996.1	99.8%	100%

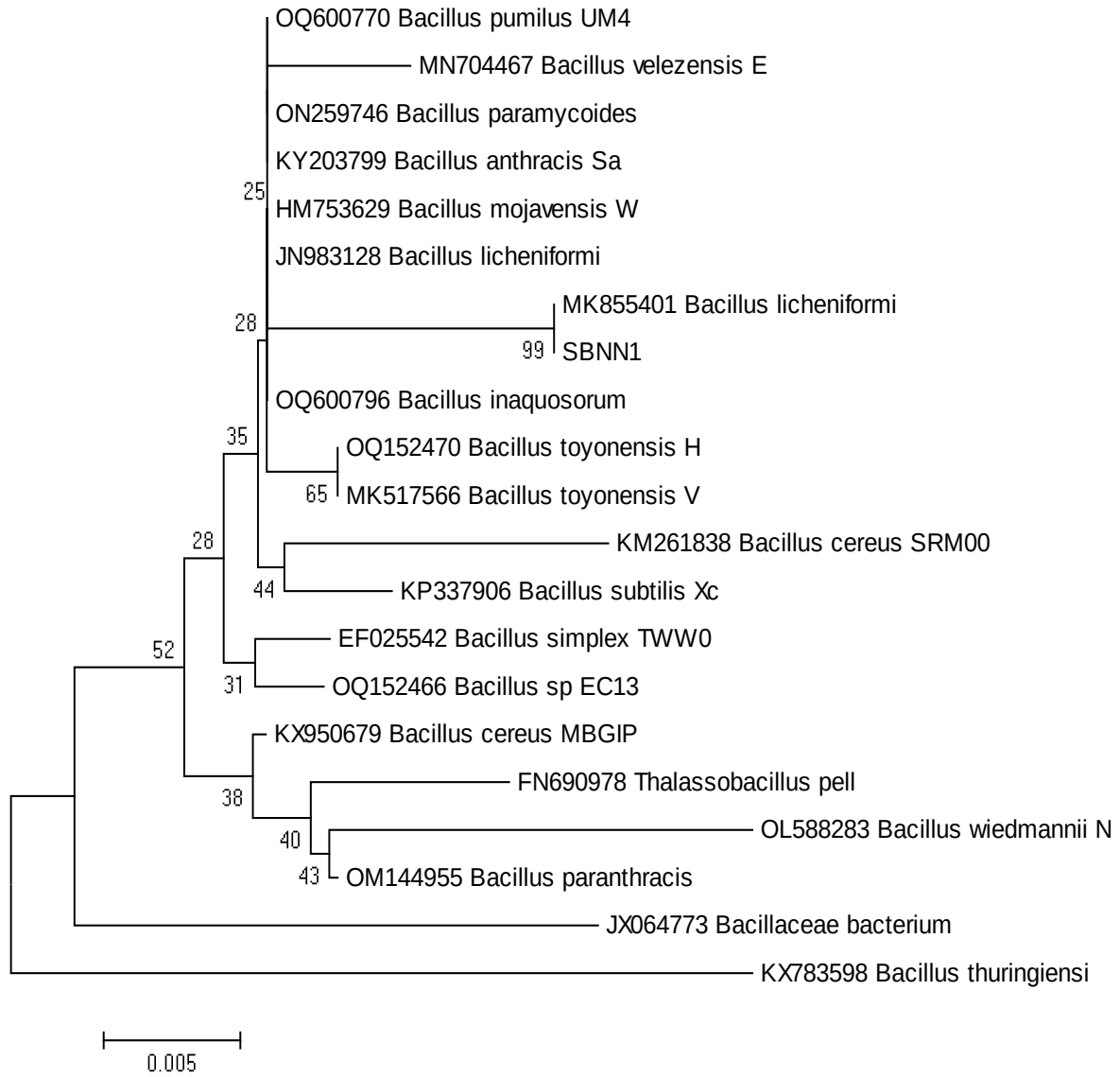

Figure 02: Neighbor-joining phylogenetic tree depicting the evolutionary relationship between Bacillus licheniformis SBNN1 (GenBank Accession No. LC814576) and other Bacillus species.

CACTTACAGATGGACCCGCGGCGCATTAGCTAGTTGGTGAGGTAACGGCTCACCAAGGCG
ACGATGCGTAGCCGACCTGAGAGGGTGATCGGCCACACTGGGACTGAGACACGGCCCAG
ACTCCTACGGGAGGCAGCAGTAGGGAATCTTCCGCAATGGACGAAAGTCTGACGGAGCA
ACGCCGCGTGAGTGATGAAGGTTTTCGGATCGTAAAACTCTGTTGTTAGGGAAGAACAAG
TACCGTTCGAATAGGGCGGTACCTTGACGGTACCTAACCAGAAAGCCACGGCTAACTACG
TGCCAGCAGCCGCGGTAATACGTAGGTGGCAAGCGTTGTCCGGAATTATTGGGCGTAAAG
CGCGCGCAGGCGGTTTCTTAAGTCTGATGTGAAAGCCCCCGGCTCAACCGGGGAGGGTCA
TTGGAAACTGGGGAACTTGAGTGCAGAAGAGGAGAGTGGAATTCCACGTGTAGCGGTGA
AATGCGTAGAGATGTGGAGGAACACCAGTGGCGAAGGCGACTCTCTGGTCTGTAACTGAC
GCTGAGGCGCGAAAGCGTGGGGAGCGAACAGGATTAGATACCCTGGTAGTCCACGCCGTA
AACGATGAGTGCTAAGTGTTAGAGGGTTTCCGCCCTTTAGTGCTGCAGCAAACGCATTAA
GCACTCCGCCTGGGGAGTACGGTCGCAAGACTGAAACTCAAAGGAATTGACGGGGGCCC
GCACAAGCGGTGGAGCATGTGGTTTAATTCGAAGCAACGCGAAGAACCTTACCAGGTCTT
GACATCCTCTGACAACCCTAGAGATAGGGCTTCCCCTTCGGGGGCAGAGTGACAGGTGGT
GCATGGTTGTCGTCAGCTCGTGTCGTGAGATTTGGGTTAAGTCCCGCAACGAGCGCAACC
CTTGATCTTAGTTGCCAGCATTCAGTTGGGCACTCTAAGGTGACTGCCGGTGCAAACCGG
AGGAAGGTGGGGATGACGTCAAATCATCATGCCCCTTATGACCTGGGCTACACACGTGCTA
CAATGGGCAGACAAAGGGCAGCGAAGCCGCGAGGCTAAGCCAATCCCACAAATCTGTTC
TCAGTTCGGATCGCAGTCTGCAACTCGACTGCGTGAAGCTGGAATCGCTAGTAATCGCGG
ATCAGCATGCCGCGGTGAATACGTTCCCGGGCCTTGTACACACCGCCCGTCACACCACGA
GAGTTTGTAACACCCGAAGTCGGTGAGGTAACCTTTTGGAGCCAGCCGCCGAAGGTGGG
ACAGATGATTGGGGTGAAGTCGTAACAAGGTAGCCGTATCGGAAGGTGCGGCTGGATCAC
CTCCTTT

Figure 03: 16S rRNA Gene Sequence of Bacillus licheniformis SBNN1 for Phylogenetic Analysis

2. Biosynthesis of Silver Nanoparticles

AgNP formation was visually confirmed by the reaction mixture changing from pale yellow to dark brown within 24-48 hours (Figure 04). This color change corresponds to silver ion reduction. UV–Vis analysis (Table 2) showed the development of a strong SPR peak at 430 nm by 48 hours, confirming AgNP formation [21]. These observations are consistent with previous studies of bacterial AgNP synthesis [6, 7]. The results suggest that B. licheniformis secretes biomolecules (e.g. proteins, enzymes) that mediate the reduction of Ag^{+} to Ag^{0}, leading to nanoparticle formation [6].

Table 02: UV–Visible Spectroscopy Data of Synthesized Silver Nanoparticles

Sample Code	Wavelength Range (nm)	Peak Absorbance (nm)	Color Observation	Inference
AgNP-BL	300–700	~430	Brownish-yellow	SPR indicative of AgNP formation

3. UV–Visible Spectroscopy

The UV–Vis spectrum (400–800 nm) showed a maximum absorbance at **430 nm**, characteristic of colloidal AgNPs. This indicates the reduction of Ag^{+} ions by bacterial biomolecules and confirms nanoparticle formation (Figure 05).

4. FTIR Spectroscopy

The FTIR spectrum of AgNPs exhibited characteristic peaks at ~3432, 1630, 1384, 1102, and 618 cm^{-1} (Table 3 and Figure 06), corresponding to functional groups such as hydroxyl, amide, and carbonyl. These suggest the involvement of proteins, enzymes, and polysaccharides from B. licheniformis in the reduction and stabilization of nanoparticles.

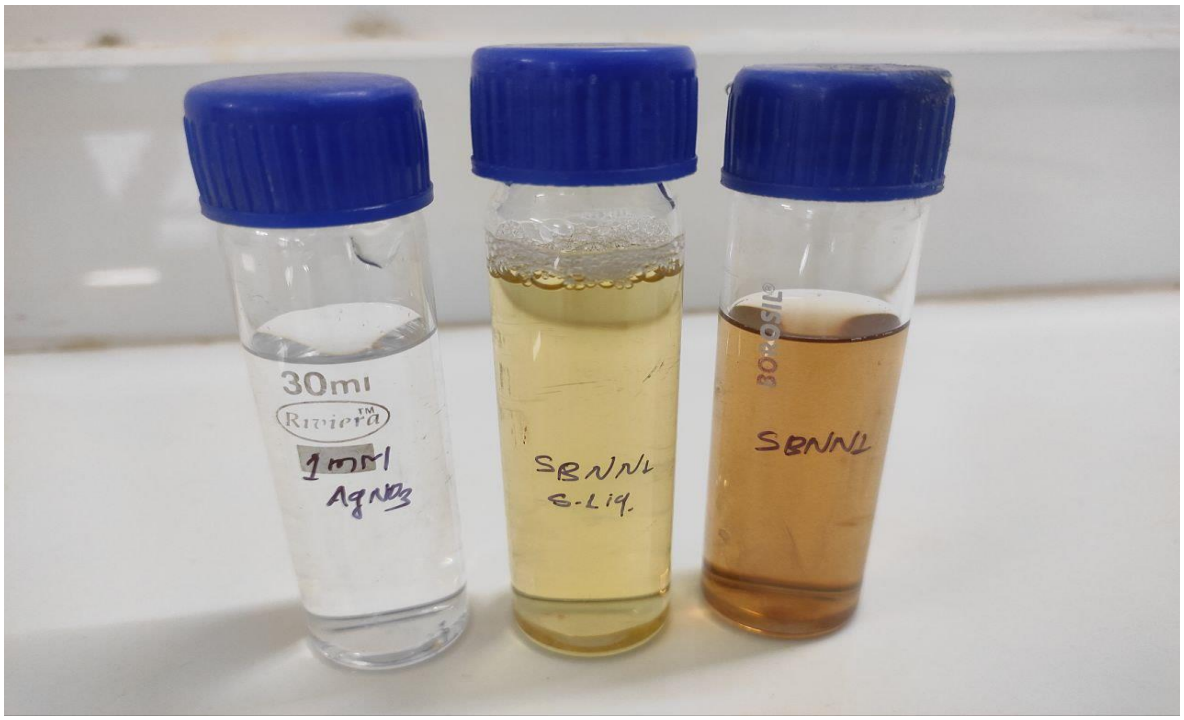

Figure 04: Biosynthesis of silver nanoparticles – visible observation.

(**Figure Illustration:** (A) 1 mM $AgNO_3$ solution (control, colourless), (B) Supernatant from Bacillus licheniformis culture before reaction (pale yellow), and (C) Reaction mixture after exposure of B. licheniformis culture supernatant to $AgNO_3$ for 48 h (brown colour indicating AgNP formation).The progressive colour change from pale yellow to brown visually confirms the synthesis of silver nanoparticles, attributable to surface plasmon resonance.)

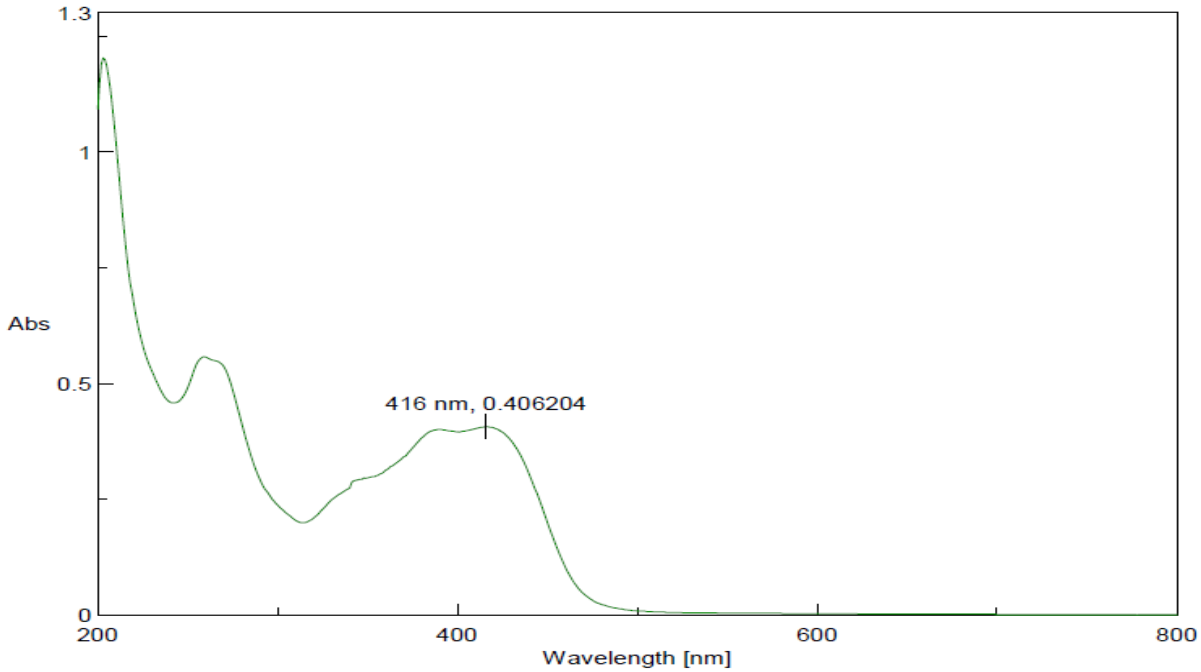

Figure 05: UV–Visible Spectroscopy of Bioinspired Silver Nanoparticles from Bacillus licheniformis

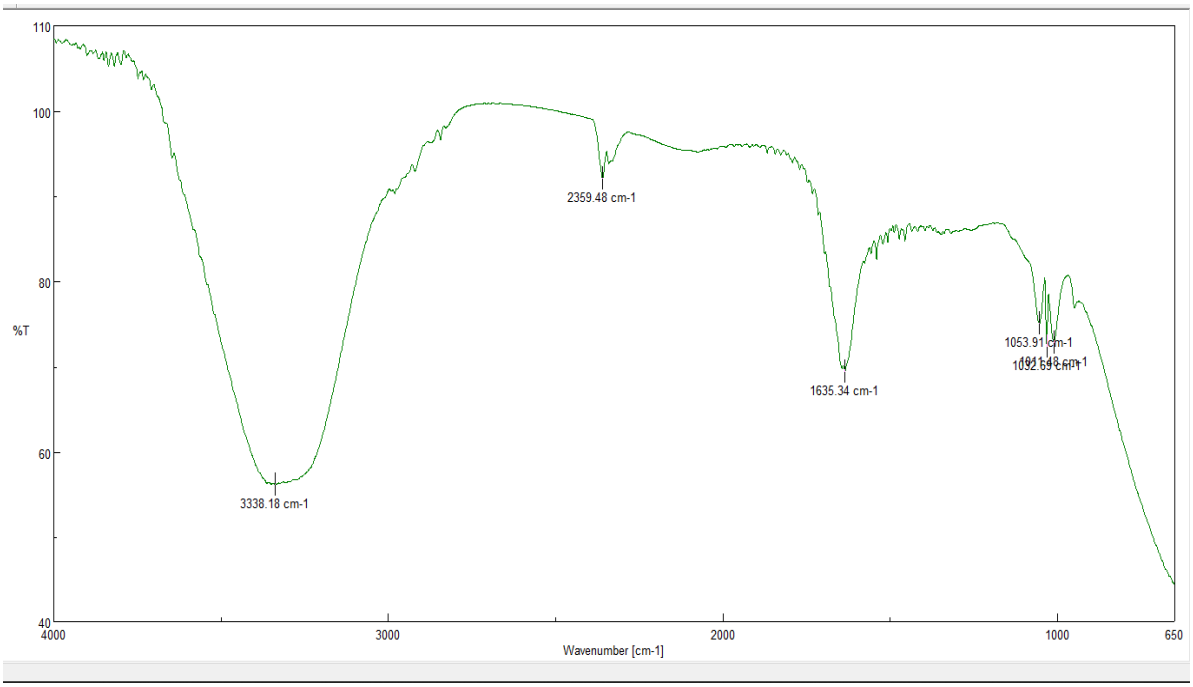

Figure 06: FTIR Spectroscopy of Bioinspired Silver Nanoparticles from Bacillus licheniformis

Table 03: FTIR Spectroscopy Data of AgNPs Synthesized by Bacillus licheniformis

Peak Position (cm^{-1})	Functional Group Assignment	Probable Biomolecular Origin
~3432	O–H / N–H stretching	Hydroxyl/amine groups (proteins)
~1630	C=O stretching (Amide I)	Peptide bonds in proteins
~1384	C–N stretching	Aromatic amines
~1102	C–O stretching	Alcohols, esters, or polysaccharides
~618	Metal–O bond or C–Cl stretch	Ag–O interaction

5. Morphology and Structure

TEM imaging revealed that the AgNPs were predominantly spherical, with a uniform size distribution ranging from 20–30 nm (Table 4, Figure 07). The particles were well-dispersed with minimal agglomeration.

Table 04: Characterization Summary of Bioinspired AgNPs

Characterization Parameter	Observation	Technique Used
Appearance	Brownish-black solution	Visual Observation
Surface Plasmon Peak	~430 nm	UV–Visible Spectroscopy
Size	20–30 nm	Transmission Electron Microscopy (TEM)
Shape	Predominantly spherical	TEM
Crystallinity	FCC lattice with peaks at 2θ: 38.2°, 44.4°, 64.6°, 77.6°	XRD
Functional Groups	–OH, –NH, –CO	FTIR
Thermal Property	Exothermic peak at ~102.25 °C, ΔH = –3063.5 J/g	DSC

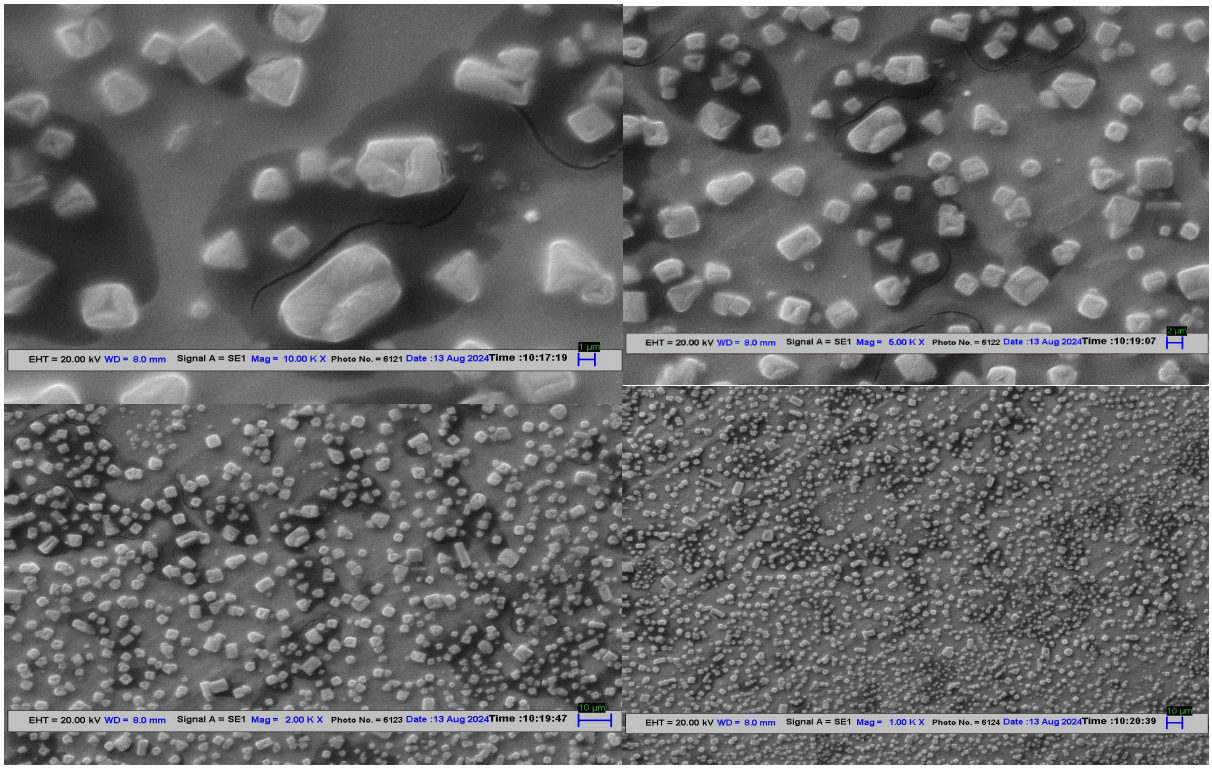

Figure 07: Transmission electron microscopy (TEM) image showing spherical AgNPs with size distribution ranging from 20–30 nm and minimal agglomeration.

6. Crystallographic Analysis

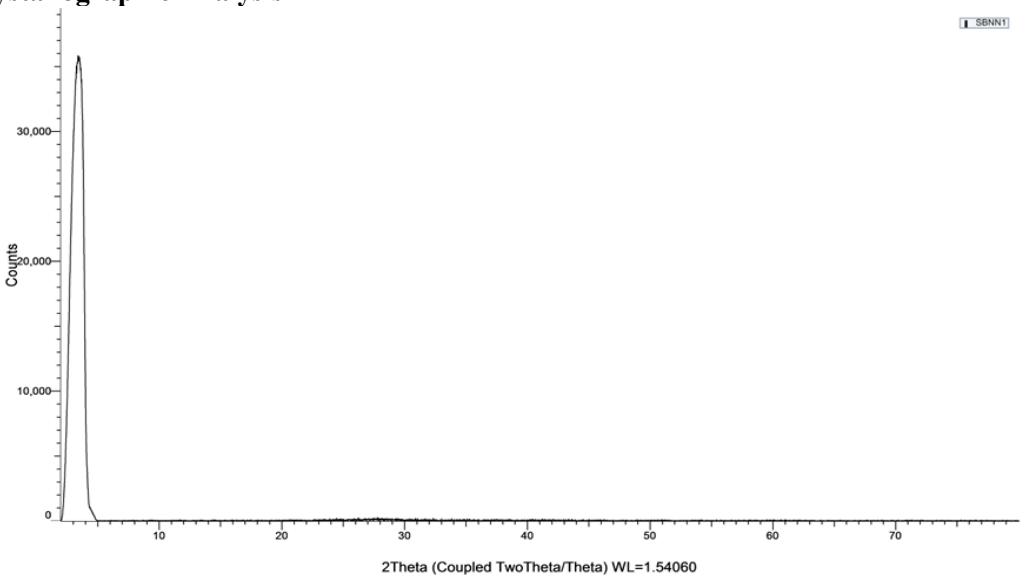

Figure 08: X-ray diffraction (XRD) pattern of AgNPs showing characteristic peaks at 2θ values corresponding to (111), (200), (220), and (311) planes of face-centered cubic (FCC) silver.

XRD patterns revealed characteristic peaks at 2θ = 38.2°, 44.4°, 64.6°, and 77.6°, corresponding to the (111), (200), (220), and (311) planes of FCC silver, respectively [13,21]. These peaks confirm the crystalline nature of the nanoparticles. TEM images (figure 08) indicated minimal agglomeration, consistent with efficient capping by biomolecules secreted by B. licheniformis. The size and morphology agree with reports that microbial synthesis yields well-defined AgNPs [3, 14].

7. Thermal Characterization

Differential Scanning Calorimetry (DSC) analysis exhibited a sharp exothermic peak at ~102.25°C with enthalpy change ΔH = –3063.50 J/g (Table 5 and Figure 09), attributed to the decomposition of organic capping agents, indicating thermal stability and uniform biomolecule coating [9].

Table 05: Comparative features of green vs. chemical synthesis of AgNPs

Feature	Green Synthesis (B. licheniformis)	Chemical Synthesis
Reducing Agent	Enzymes/Proteins	$NaBH_4$ or Citrate
Stabilizer	Natural biomolecules	Synthetic polymers
Energy Requirement	Ambient	High (often requires heating)
Toxicity	Minimal	High
Environmental Impact	Eco-friendly	Hazardous waste

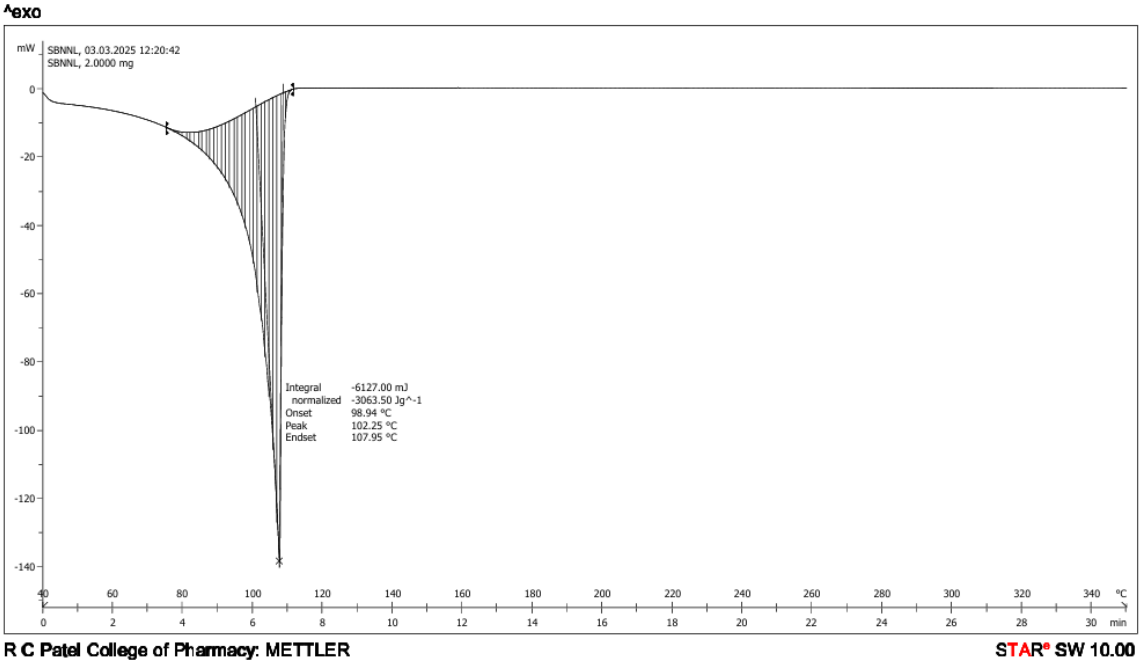

Figure 09: DSC thermogram showing an exothermic transition at 102.25 °C with ΔH = –3063.50 J/g, attributed to the degradation of organic capping agents.

8. Antibacterial Efficacy of Silver Nanoparticles via Well-Diffusion Assay

The antibacterial potential of silver nanoparticles (AgNPs) was evaluated against four clinically relevant, wound-associated bacterial pathogens: Staphylococcus aureus, Pseudomonas aeruginosa, Escherichia coli, and Klebsiella pneumoniae, using the agar well-diffusion method (19, 20, 22, 23). The diameter of the zones of inhibition (ZOI), measured in millimeters, served as an indicator of antimicrobial activity at different AgNP concentrations (200, 300, 400, and 500 µg/mL), along with a control group lacking AgNPs.

A dose-dependent enhancement in antibacterial activity was observed across all bacterial strains tested. Among them, Staphylococcus aureus showed the highest susceptibility, with the ZOI increasing from 5 mm (control) to 12 mm at 500 µg/mL of AgNPs, indicating potent inhibition. Klebsiella pneumoniae also exhibited notable sensitivity, with the ZOI expanding from 4 mm (control) to 10 mm at the highest concentration. Pseudomonas aeruginosa, known for its robust resistance mechanisms, exhibited a comparatively lower but still progressive inhibition (2 mm at control to 9 mm at 500 µg/mL), suggesting that AgNPs can overcome some resistance barriers.

Escherichia coli demonstrated moderate susceptibility, with the ZOI increasing from 4 mm (control) to 10 mm at the highest concentration. These results (Table 6 and Figure10) corroborate earlier findings highlighting the broad-spectrum antimicrobial activity of silver nanoparticles (23, 24). The variation in sensitivity among Gram-positive and Gram-negative bacteria underscores the potential of AgNPs as an alternative or adjunct to conventional antibiotics, especially in the context of multidrug-resistant infections.

Table 06: Zone of Inhibition (mm) Exhibited by AgNPs at Varying Concentrations

Organism	Zone of Inhibition in mm				
	Control	200 µg/mL	300 µg/mL	400 µg/mL	500 µg/mL
Staphylococcus aureus	5	7	8	9	12
Pseudomonas aeruginosa	2	6	7	8	9
Escherichia coli	4	5	6	8	10
Klebsiella pneumoniae	4	6	8	9	10

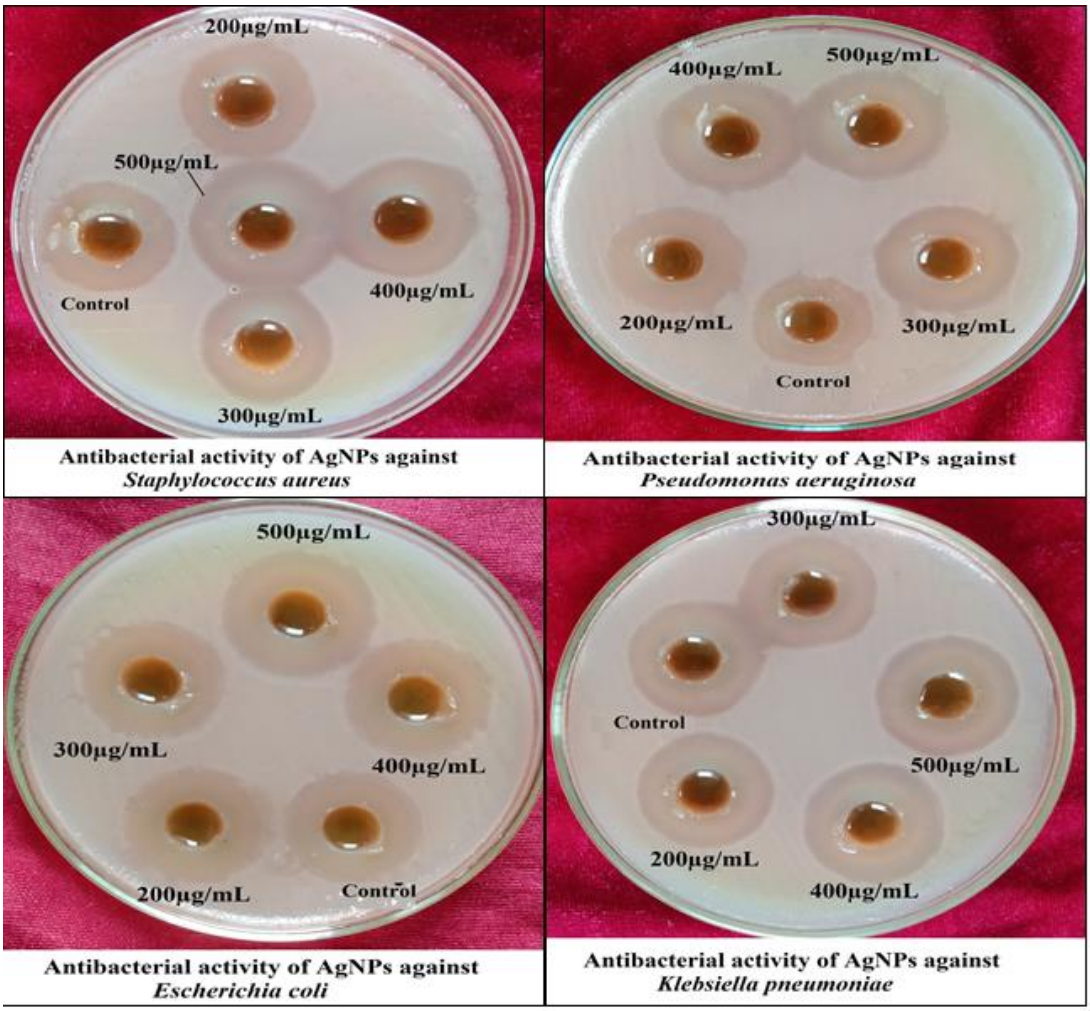

Figure 10: Agar plates showing zones of inhibition for S. aureus, E. coli, P. aeruginosa, and K. pneumoniae after treatment with biosynthesized AgNPs.

Mechanism of Antimicrobial Action [24, 25]:

AgNPs are known to exert antimicrobial effects via multiple mechanisms

- Generation of reactive oxygen species (ROS), leading to oxidative stress in bacterial cells.
- Disruption of the bacterial cell membrane and interference with intracellular processes such as DNA replication and protein synthesis.
- Binding to thiol groups in proteins, causing functional disruptions.

The present study demonstrated that B. licheniformis-synthesized AgNPs are potent antimicrobial agents. The natural capping biomolecules from the bacteria may enhance the nanoparticles' bioactivity and biocompatibility. These AgNPs may thus offer advantages over chemically synthesized particles in biomedical applications.

DISCUSSION

The present study demonstrates the eco-friendly synthesis of silver nanoparticles (AgNPs) using Bacillus licheniformis isolated from rhizosphere soil. The successful isolation and 16S rRNA-based molecular identification of the bacterium (99.8% identity) confirmed its suitability as a microbial nanofactory. Rhizospheric B. licheniformis was able to reduce silver ions (Ag^{+}) to elemental silver (Ag^{0}), evident from the rapid color change of the reaction mixture to brown and the surface plasmon resonance (SPR) peak at ~430 nm, confirming nanoparticle formation [2, 6].

The biological reduction of silver ions is mediated by a diverse array of biomolecules secreted by Bacillus species, including enzymes, amino acids, peptides, and polysaccharides (3,9). FTIR spectral data in this study revealed characteristic peaks at ~3432, 1630, and 1384 cm^{-1}, indicating the involvement of –OH, amide, and C–N functional groups, which likely participate in both the reduction and stabilization of AgNPs [1].

Transmission electron microscopy (TEM) revealed uniformly distributed, predominantly spherical nanoparticles ranging from 20–30 nm in size, consistent with the size range reported for biologically synthesized AgNPs (14). X-ray diffraction (XRD) analysis showed distinct peaks corresponding to the (111), (200), (220), and (311) planes of the face-centered cubic (FCC) silver structure, affirming the crystalline nature of the nanoparticles [13].

Furthermore, differential scanning calorimetry (DSC) showed an exothermic peak at ~102.25 °C, attributed to the decomposition of organic capping agents, suggesting a uniform capping layer and thermal stability. The presence of natural biomolecules on the nanoparticle surface is thought to enhance their colloidal stability and biological activity [5].

Importantly, the silver nanoparticles (AgNPs) demonstrated concentration-dependent antimicrobial activity against both Gram-positive (Staphylococcus aureus) and Gram-negative bacteria (Pseudomonas aeruginosa, Escherichia coli, and Klebsiella pneumoniae). The zones of inhibition ranged from 2 mm (P. aeruginosa, control) to 12 mm (S. aureus, 500 µg/mL), highlighting the broad-spectrum efficacy of AgNPs. These findings are consistent with previous reports on the potent antibacterial potential of silver nanoparticles against diverse microbial species [24, 25, 26]. The bactericidal action of AgNPs involves multiple mechanisms including disruption of cell membranes, inhibition of DNA replication, protein denaturation, and the generation of reactive oxygen species (ROS) [13, 21].

Notably, the green synthesis method used in this study offers several advantages over chemical methods, including reduced toxicity, lower energy consumption, and the use of renewable biological resources [4, 7]. Comparative evaluation (Table 5) highlights the environmental and functional superiority of green synthesis using B. licheniformis.

In summary, this work underscores the potential of rhizospheric Bacillus licheniformis as a sustainable and efficient biological system for synthesizing biofunctional AgNPs. The synthesized nanoparticles demonstrated desirable physicochemical features and promising antimicrobial efficacy, paving the way for their application in biomedicine, agriculture, and environmental remediation.

CONCLUSION

The present study successfully demonstrates the green synthesis of silver nanoparticles (AgNPs) using Bacillus licheniformis isolated from rhizospheric soil. The biosynthesis process is eco-friendly, cost-effective, and capable of producing stable, spherical AgNPs ranging from 20–30 nm in size. Characterization by UV–Vis, FTIR, XRD, TEM, and DSC confirmed the optical, structural, and

thermal stability of the nanoparticles, while FTIR analysis revealed the involvement of bacterial biomolecules in nanoparticle reduction and capping. Moreover, the biosynthesized AgNPs exhibited potent antimicrobial activity against both Gram-positive and Gram-negative multidrug-resistant pathogens, highlighting their potential as effective biocidal agents. Compared to conventional chemical synthesis, this biological route offers several advantages, including reduced toxicity, lower environmental impact, and natural functionalization. This study underscores the potential of Bacillus licheniformis as a sustainable microbial platform for nanoparticle production. Future research should focus on optimizing large-scale production, investigating in vivo efficacy and toxicity, and expanding the scope of biomedical and environmental applications.

ACKNOWLEDGEMENT

We sincerely thanks to Dr. Rahul More, Department of Microbiology, Dayanand Science College, Latur for his expert supervision and guidance throughout our study and Centre for Research in Pharmaceutical Sciences (CRPS), Channabasweshwar Pharmacy College (Degree), Latur for providing necessary research facility throughout this research.

REFERENCES

1. Ahmed, S., Ahmad, M., Swami, B. L., & Ikram, S. (2016). Green synthesis of silver nanoparticles using Azadirachta indica aqueous leaf extract. Journal of Radiation Research and Applied Sciences, 9(1), 1–7. https://doi.org/10.1016/j.jrras.2015.06.006
2. Rai, M., Yadav, A., & Gade, A. (2009). Silver nanoparticles as a new generation of antimicrobials. Biotechnology Advances, 27(1), 76–83. https://doi.org/10.1016/j.biotechadv.2008.09.002
3. Iravani, S. (2011). Green synthesis of metal nanoparticles using plants. Green Chemistry, 13(10), 2638–2650. https://doi.org/10.1039/C1GC15386B
4. Anastas, P. T., & Eghbali, N. (2010). Green chemistry: Principles and practice. Chemical Society Reviews, 39(1), 301–312. https://doi.org/10.1039/B918763B
5. Shah, M., Fawcett, D., Sharma, S., Tripathy, S. K., & Poinern, G. E. J. (2015). Green synthesis of metallic nanoparticles via biological entities. Materials, 8(11), 7278–7308. https://doi.org/10.3390/ma8115377
6. Mittal, A. K., Chisti, Y., & Banerjee, U. C. (2013). Biosynthesis of silver nanoparticles: Mechanisms and therapeutic potential. Journal of Colloid and Interface Science, 415, 39–47. https://doi.org/10.1016/j.jcis.2013.01.018
7. Singh, P., Kim, Y. J., Zhang, D., & Yang, D. C. (2016). Biological synthesis of nanoparticles from plants and microorganisms. Trends in Biotechnology, 34(7), 588–599. https://doi.org/10.1016/j.tibtech.2016.02.006
8. Mukherjee, P., Ahmad, A., Mandal, D., Senapati, S., Sainkar, S. R., Khan, M. I., ... & Sastry, M. (2001). Fungus-mediated synthesis of silver nanoparticles and their immobilization in the mycelial matrix: A novel biological approach to nanoparticle synthesis. Angewandte Chemie International Edition, 40(19), 3585–3588. https://doi.org/10.1002/1521-3773(20011001)40:19<3585::AID-ANIE3585>3.0.CO;2-K
9. Narayanan, K. B., & Sakthivel, N. (2010). Biological synthesis of metal nanoparticles by microbes. Advances in Colloid and Interface Science, 156(1-2), 1–13. https://doi.org/10.1016/j.cis.2010.02.001
10. Gopalakrishnan, S., Humayun, P., Kiran, B. K., Kannan, I. G., Vidya, M. S., & Deepthi, K. (2011). Plant growth-promoting rhizobacteria for sustainable agricultural practices. Biological Control, 57(2), 119–129. https://doi.org/10.1016/j.biocontrol.2011.03.002
11. Khatami, M., Alijani, H. Q., Nejad, F. M., & Zafarnia, N. (2018). Core–shell nanoparticles: Greener synthesis using natural plant products. Applied Sciences, 8(3), 411. https://doi.org/10.3390/app8030411
12. Hayat, R., Ali, S., Amara, U., Khalid, R., & Ahmed, I. (2010). Soil beneficial bacteria and their role in plant growth promotion: A review. Annals of Microbiology, 60(4), 579–598. https://doi.org/10.1007/s13213-010-0117-1
13. Durán, N., Marcato, P. D., De Souza, G. I. H., Alves, O. L., & Esposito, E. (2011). Mechanistic aspects in the biogenic synthesis of extracellular metal nanoparticles by peptides, bacteria, fungi, and plants. Applied Microbiology and Biotechnology, 90(5), 1609–1624. https://doi.org/10.1007/s00253-011-3249-8
14. Firdhouse, M. J., & Lalitha, P. (2015). Biosynthesis of silver nanoparticles and its applications. Journal of Nanotechnology, 2015, 1–18. https://doi.org/10.1155/2015/829526
15. Williams, S. T., Sharpe, M. E., & Holt, R. J. (1989). Principles of Microbiology. McGraw-Hill Education.

16. Cappuccino, J. G., & Sherman, N. (2014). Microbiology: A Laboratory Manual (10th ed.). Pearson Education.
17. Cowan, S. T., & Steel, K. J. (1993). Manual for the Identification of Medical Bacteria (3rd ed.). Cambridge University Press.
18. Janda, J. M., & Abbott, S. L. (2007). 16S rRNA gene sequencing for bacterial identification in the diagnostic laboratory: Pluses, perils, and pitfalls. Journal of Clinical Microbiology, 45(9), 2761–2764. https://doi.org/10.1128/JCM.01228-07
19. Balouiri, M., Sadiki, M., & Ibnsouda, S. K. (2016). Methods for in vitro evaluating antimicrobial activity: A review. Journal of Pharmaceutical Analysis, 6(2), 71–79. https://doi.org/10.1016/j.jpha.2015.11.005
20. Clinical and Laboratory Standards Institute (CLSI). (2021). Performance standards for antimicrobial susceptibility testing (31st ed.). CLSI Supplement M100.
21. Baker, C., Pradhan, A., Pakstis, L., Pochan, D. J., & Shah, S. I. (2005). Synthesis and antibacterial properties of silver nanoparticles. Journal of Nanoscience and Nanotechnology, 5(2), 244–249. https://doi.org/10.1166/jnn.2005.034
22. Franci, G., Falanga, A., Galdiero, S., Palomba, L., Rai, M., Morelli, G., & Galdiero, M. (2015). Silver nanoparticles as potential antibacterial agents. Molecules, 20(5), 8856–8874. https://doi.org/10.3390/molecules20058856
23. Durán, N., Marcato, P. D., De Souza, G. I. H., Alves, O. L., & Esposito, E. (2007). Silver nanoparticles: A new view on mechanistic aspects on antimicrobial activity. Nanomedicine: Nanotechnology, Biology and Medicine, 3(2), 221–229. https://doi.org/10.1016/j.nano.2007.02.003
24. Pal, S., Tak, Y. K., & Song, J. M. (2007). Does the antibacterial activity of silver nanoparticles depend on the shape of the nanoparticle? A study of the gram-negative bacterium Escherichia coli. Applied and Environmental Microbiology, 73(6), 1712–1720. https://doi.org/10.1128/AEM.02218-06
25. Li, X., Robinson, S. M., Gupta, A., Saha, K., Jiang, Z., Moyano, D. F., ... & Rotello, V. M. (2010). Functional gold nanoparticles as potent antimicrobial agents against multi-drug-resistant bacteria. ACS Nano, 8(10), 10682–10686. https://doi.org/10.1021/nn503876k
26. Jain, D., Daima, H. K., Kachhwaha, S., & Kothari, S. L. (2009). Synthesis of plant-mediated silver nanoparticles using Papaya fruit extract and evaluation of their antimicrobial activities. Journal of Biomedical Nanotechnology, 5(1), 93–98. https://doi.org/10.1166/jbn.2009.1055